

## Detention Times of Microswimmers Close to Surfaces: Influence of Hydrodynamic Interactions and Noise

Konstantin Schaar,<sup>1,2,3</sup> Andreas Zöttl,<sup>1</sup> and Holger Stark<sup>1</sup>

<sup>1</sup>*Institut für Theoretische Physik, Technische Universität Berlin, Hardenbergstrasse 36, 10623 Berlin, Germany*

<sup>2</sup>*Institut für Theoretische Biologie, Humboldt Universität Berlin, Invalidenstrasse 43, 10115 Berlin, Germany*

<sup>3</sup>*Robert Koch-Institut, Seestrassen 10, 13353 Berlin, Germany*

(Received 2 December 2014; published 15 July 2015)

After colliding with a surface, microswimmers reside there during the detention time. They accumulate and may form complex structures such as biofilms. We introduce a general framework to calculate the distribution of detention times using the method of first-passage times and study how rotational noise and hydrodynamic interactions influence the escape from a surface. We compare generic swimmer models to the simple active Brownian particle. While the respective detention times of source dipoles are smaller, the ones of pullers are larger by up to several orders of magnitude, and pushers show both trends. We apply our results to the more realistic squirmer model, for which we use lubrication theory, and validate them by simulations with multiparticle collision dynamics.

DOI: [10.1103/PhysRevLett.115.038101](https://doi.org/10.1103/PhysRevLett.115.038101)

PACS numbers: 47.63.Gd, 47.63.mf, 87.10.Mn

Biological microswimmers such as bacteria are omnipresent in our everyday life. At the micron scale their locomotion in an aqueous environment is determined by low-Reynolds-number hydrodynamics and influenced by thermal and intrinsic biological noise [1,2]. In real environments such as the human body [3] or the ocean [4,5] microorganisms swim in the presence of soft or solid boundaries where they may form complex aggregates such as biofilms [6]. This letter develops a general approach for investigating the fundamental and biologically relevant question of how long a swimming microorganism resides at bounding surfaces by accounting for both hydrodynamic swimmer-wall interactions and noise.

To develop an understanding for the accumulation and the dynamics of microorganisms near walls, several important aspects have been investigated recently: swimmer-wall hydrodynamic interactions [7–10], thermal and intrinsic noise [7,11], cilia- and flagella-wall interactions [12], bacterial tumbling [13], and buoyancy [14]. Whether stochastic motion or swimmer-wall hydrodynamic interactions determine the reorientation of microswimmers at a surface and how they both influence the bacterial distribution between parallel plates has been discussed controversially [7,8,11]. Hydrodynamic interactions trap bacteria at surfaces [8,15], force them to swim in circles [16], or even suppress bacterial tumbling [13]. However, nontumbling bacteria [7,11] or elongated artificial microswimmers [17] use rotational noise to escape from surfaces.

Artificial microswimmers such as active Janus particles or squirmers, which are driven by a surface velocity field, have been studied in front of a no-slip wall both in experiments [18,19] and by theoretical models. The latter either include hydrodynamic interactions [15,20–24] or only consider active Brownian particles [18,25–28].

An important prerequisite for the observed accumulation near walls are the relatively large times microswimmers reside at a surface before leaving it [17,18]. In this article we call these swimmer-wall contact times detention times and calculate their distributions near a plane no-slip surface based on the method of first-passage times [29]. For generic microswimmers we demonstrate that hydrodynamic interactions, relative to pure rotational noise, can either increase the mean detention time by several orders of magnitude or also decrease it.

At low Reynolds number the motion of an axisymmetric microswimmer with orientation  $\mathbf{e}$  in the presence of bounding surfaces is governed by the Langevin equations

$$\begin{aligned}\dot{\mathbf{r}} &= \mathbf{v}_A + \mathbf{v}_{HI} + \mathbf{v}_N + \dots, \\ \dot{\mathbf{e}} &= \boldsymbol{\Omega} \times \mathbf{e} \quad \text{with} \quad \boldsymbol{\Omega} = \boldsymbol{\Omega}_{HI} + \boldsymbol{\Omega}_N + \dots,\end{aligned}\quad (1)$$

which account for the stochastic dynamics of position  $\mathbf{r}$  and orientation  $\mathbf{e}$ . Here we only consider the influence of the activity of the swimmer ( $\mathbf{v}_A = U\mathbf{e}$  with bulk swimming velocity  $U$ ), hydrodynamic interactions with the surface (HI), and noise ( $N$ ). However, our approach can, in principle, be used for any dynamics which is of the form of Eq. (1) and also include, e.g., steric or electrostatic interactions as well as external fluid flow.

We consider a spherical microswimmer, moving on a smooth trajectory, which reaches the wall at time  $t_0$  with an angle  $\theta_0$  against the surface normal (see Fig. 1 and a typical trajectory in the Supplemental Material [30]). This occurs at Péclet number  $Pe = UR/D_t \gg 1$ , where  $R$  is the radius and  $D_t$  the translational diffusion coefficient of the swimmer. Typical values are  $Pe \gtrsim 10^2$  for bacteria,  $Pe \gtrsim 10^3$  for sperm cells and  $Pe \gtrsim 10^4$  for *Chlamydomonas*. The swimmer stays at a height  $h \approx R$ , so we neglect

translational motion in the following [31]. The swimming direction  $\mathbf{e}$  diffuses on the unit sphere but also drifts with angular velocity  $\mathbf{\Omega}_{\text{HI}} = \mathbf{\Omega}_{\text{HI}}\mathbf{e}_\phi$ . Once the swimming direction has reached the escape angle  $\theta^*$ , to be defined below for each swimmer type, the microswimmer leaves the surface at time  $t^*$ . This stochastic process is described by the Smoluchowski equation  $\partial_t P = \mathcal{L}P = (-\mathcal{R} \cdot \mathbf{\Omega}_{\text{HI}} + D_r \mathcal{R}^2)P$ , where  $\mathcal{R} = \mathbf{e} \times \nabla_{\mathbf{e}}$  is the rotation operator and  $D_r$  the rotational diffusion constant [26,32].

Rotational diffusion along the azimuthal angle  $\phi$  does not influence the escape from the surface and it is sufficient to consider the conditional probability  $p(\theta, t^*|\theta_0, t_0) = \int_0^{2\pi} d\phi_0 \int_0^{2\pi} d\phi P(\theta, \phi, t^*|\theta_0, \phi_0, t_0)$ . To calculate the distribution of detention times at the surface, we use the Fokker-Planck approach of first-passage problems [29]. The integrated probability  $g(\theta^*, t|\theta_0) = \int_{\theta^*}^{\pi} p(\theta, t^*|\theta_0, t_0) \sin\theta d\theta$  for finding the swimming direction in the angular interval  $[\theta^*, \pi]$  at time  $t = t^* - t_0$  obeys the adjoint Smoluchowski equation (see Ref. [30])

$$\partial_t g(\theta^*, t|\theta_0) = \mathcal{L}^+(\theta_0)g(\theta^*, t|\theta_0), \quad (2)$$

with  $\mathcal{L}^+(\theta_0) = \Omega(\theta_0)\partial_{\theta_0} + D_r\partial_{\theta_0}^2$ , where  $\Omega(\theta_0) = \Omega_{\text{HI}}(\theta_0) + D_r \cot\theta_0$  is an effective angular drift velocity. To solve it, one uses at  $\theta_0 = \pi$  reflective

$[\partial_{\theta_0} g(\theta^*, t|\theta_0)|_{\pi} = 0]$  and at  $\theta_0 = \theta^*$  absorbing  $[g(\theta^*, t|\theta^*) = 0]$  boundary conditions. Now,  $-\partial_t g(\theta^*, t|\theta_0)dt$  is the probability to leave the surface with escape angle  $\theta^*$  at time  $t$  in the time interval  $dt$ , so

$$f(\theta^*, t|\theta_0) = -\partial_t g(\theta^*, t|\theta_0) \quad (3)$$

denotes the distribution of detention times  $t = t^* - t_0$  for being trapped at the surface (DTD).

To investigate how hydrodynamic interactions compared to pure rotational noise influence the detention time, we calculate the DTD  $f(\theta^*, t|\theta_0)$  for several model microswimmers by numerically solving Eq. (2) and using Eq. (3). From here on, we always rescale time by the ballistic time scale  $\tau_s = R/U$  and introduce the persistence number  $\text{Pe}_r = (2D_r\tau_s)^{-1}$ . Since  $(2D_r)^{-1}$  is the orientational correlation time,  $\text{Pe}_r \gg 1$  means directed swimming [11,33]. Typical values are  $\text{Pe}_r \gtrsim 100$  for sperm cells [34] and nontumbling *E. coli* [7], or  $\text{Pe}_r \approx 25$  for *Chlamydomonas* [7].

First, we consider a spherical active Brownian particle (ABP) with  $\mathbf{\Omega}_{\text{HI}} = 0$  near a surface [26,28]. The escape angle is simply  $\theta^* = \pi/2$ . From the known propagator of free rotational diffusion [35], one can determine  $g(\theta^*, t|\theta_0)$  and ultimately the DTD becomes

$$f\left(\frac{\pi}{2}, t|\theta_0\right) = \frac{\pi}{2\text{Pe}_r} \sum_{l=1, \text{odd}}^{\infty} (-1)^{[(l+1)/2]} e^{-l(l+1)t/(2\text{Pe}_r)} \frac{l(2l+1)}{2^{l-1}} \binom{l-1}{\frac{l-1}{2}} P_l(\cos\theta_0), \quad (4)$$

where  $P_l(\cos\theta_0)$  are Legendre polynomials. The DTD is plotted in Fig. 2(a) for  $\theta_0 = 3\pi/4$  and  $\text{Pe}_r = 10$ . The mean detention time  $T = \int_0^{\infty} t f(\theta^*, t|\theta_0) dt$  of the ABP at the surface is calculated following Ref. [29],

$$T^{\text{ABP}} = 2\text{Pe}_r \ln(1 - \cos\theta_0). \quad (5)$$

We plot  $T^{\text{ABP}}$  versus  $\theta_0$  in Fig. 2(b). Note that the most likely detention time  $t_{\text{max}}$  [see Fig. 2(c)] is much smaller compared to  $T^{\text{ABP}}$  due to the slow decay of  $f(\theta^*, t|\theta_0)$ .

Second, we consider microswimmers that generate either a force-dipole flow field of strength  $p$  or a source dipole

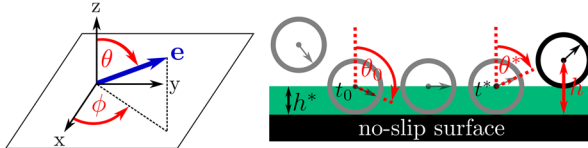


FIG. 1 (color online). Definition of coordinate system and sketch of a typical trajectory for a spherical microswimmer approaching a plane no-slip surface ( $h = h^*$ ) at time  $t_0$  and leaving the surface at  $t^*$ . The detention time at the surface is  $t^* - t_0$ .

field of strength  $q > 0$  in the surrounding fluid [2]. Examples for the first case are pushers ( $p > 0$ ) such as bacteria, or pullers ( $p < 0$ ) such as the biflagellated algae *Chlamydomonas*. Source dipoles are realized by active droplets [36] or *Paramecia* [37]. Each flow field is described by a flow singularity located in the center of

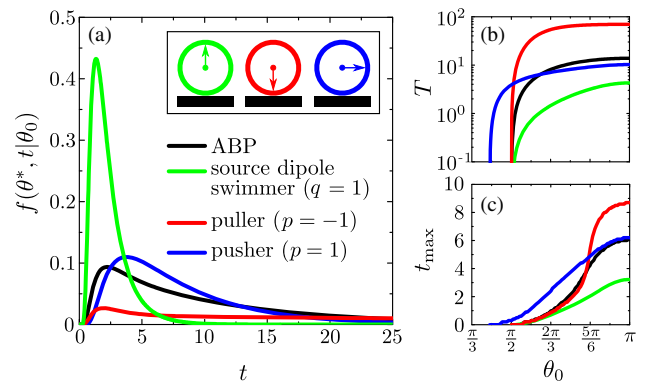


FIG. 2 (color online). (a) DTD for the ABP and source- and force-dipole swimmer with  $\text{Pe}_r = 10$  and an initial angle  $\theta_0 = 3\pi/4$ . (b) Mean detention time  $T$  versus initial angle  $\theta_0$ . (c) Most likely detention time  $t_{\text{max}}$  (maximum of  $f$ ).

the swimmer. For simplicity, we assume that the description by singularities is still valid close to the wall (see also the discussion in Refs. [7,15]). Their flow fields interact hydrodynamically with the surface and thereby generate wall-induced angular velocities  $\Omega_{\text{HI}}$  of the microswimmers. At the wall ( $h = R$ ) they read  $\Omega_{\text{HI}} = 3p \sin \theta \cos \theta / 8$  for the force dipole and  $\Omega_{\text{HI}} = -3q \sin \theta / 8$  for the source dipole, respectively [8,15,38]. The stable orientations  $\theta_s$  of our swimmer types at the wall in the absence of noise are sketched in the inset of Fig. 2(a). They are calculated from  $\Omega_{\text{HI}}(\theta_s) = 0$  and  $\partial\Omega_{\text{HI}}(\theta)/\partial\theta|_{\theta=\theta_s} < 0$ .

Hydrodynamic interactions of the source dipole ( $q > 0$ ) always rotate the swimmer away from the surface until it leaves the surface at  $\theta^* = \pi/2$ . Hence, the width of the DTD is much narrower compared to the ABP [see Fig. 2(a)]. The mean detention time  $T$  plotted in Fig. 2(b) is much smaller compared to  $T^{\text{ABP}}$  for all incoming angles  $\theta_0$  due to  $\Omega_{\text{HI}} \propto -q$  and the most likely detention time  $t_{\text{max}}$  is comparable to  $T$  [see Fig. 2(c)].

The puller ( $p < 0$ ) is rotated towards the surface by hydrodynamic interactions if  $\theta > \pi/2$  and can only escape if angular noise drives it to  $\theta < \theta^* = \pi/2$ . As a consequence, the DTD only has a weakly pronounced maximum and decays very slowly [see Fig. 2(a)]. Therefore, at  $\text{Pe}_r = 10$  the mean detention time of the puller is by an order of magnitude larger than for the ABP. We note that for biological swimmers direct flagella-wall interactions can significantly influence the reorientation at the wall. For the puller algae *Chlamydomonas*  $\Omega_{\text{steric}} > 0$ , which rotates the cell away from the surface [12] and strongly decreases the detention times compared to ABPs (see also Ref. [30]).

The situation of the pusher ( $p > 0$ ) is more complex. Because of hydrodynamic interactions it has a stable orientation parallel to the wall [ $\theta_s = \pi/2$ , see inset of Fig. 2(a)]. Since, in addition, the wall-induced velocity  $\mathbf{v}_{\text{HI}}(\theta_s)$  pushes it towards the wall, a noiseless pusher always swims at the wall [8] and  $T \rightarrow \infty$ . In the presence of noise the swimmer orientation fluctuates about its stable direction. The pusher stays trapped until the escape angle  $\theta^* < \pi/2$  is reached, where the total swimmer velocity starts to point away from the wall. Thus, the escape angle is determined by the condition  $[\mathbf{v}_A(\theta^*) + \mathbf{v}_{\text{HI}}(\theta^*)] \cdot \mathbf{e}_z = 0$ , which gives  $\theta^* = \arccos[(-4 + \sqrt{16 + 27p^2})/(9p)]$  [7,8].

Hydrodynamic interactions of the pusher with the surface can either enhance or reduce the detention time compared to an ABP. On the one hand, increasing  $p \propto \Omega_{\text{HI}}$  from zero reduces the time to reach the stable orientation and thus the time to get closer to the escape angle  $\theta^* < \pi/2$ . This can reduce the mean detention time compared to ABPs for small  $p$  as illustrated in Fig. 2(b). On the other hand, increasing  $p$  further traps the orientation more strongly at  $\theta_s = \pi/2$  and also pushes  $\theta^*$  more and more away from  $\theta_s$ . Since rotational diffusion has to compensate for both effects, the detention time increases.

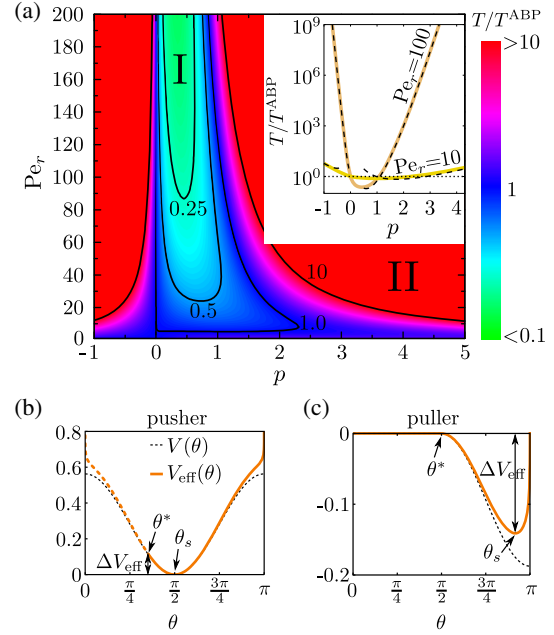


FIG. 3 (color online). (a) Mean detention time  $T/T^{\text{ABP}}$  for the force-dipole swimmer plotted versus  $p$  and  $\text{Pe}_r$  for  $\theta_0 = 3\pi/4$ . Within region I,  $T/T^{\text{ABP}} < 1$ , while in region II,  $T/T^{\text{ABP}} \gg 1$ . Inset:  $T(p)/T^{\text{ABP}}$  for two values of  $\text{Pe}_r$  and compared to Eqs. (6) and (7) (dashed lines). (b),(c) Effective angular potentials  $V_{\text{eff}}(\theta)$  and deterministic potentials  $V(\theta)$  ( $\text{Pe}_r \rightarrow \infty$ ) for a pusher (b) ( $p = 3$ ) and a puller (c) ( $p = -1$ ) at  $\text{Pe}_r = 20$ .

Figure 3(a) gives an overview of the force-dipole swimmer by plotting  $T/T^{\text{ABP}}$  in a color code versus  $\text{Pe}_r$  and  $p$ . For negative  $p$  the strong increase of  $T$  beyond  $T^{\text{ABP}}$  with increasing  $|p|$  is visible and also documented in the inset for two values of  $\text{Pe}_r$ . For small positive  $p$  and for  $\text{Pe}_r \gtrsim 5$  a clear minimum of  $T$  develops as just discussed (see also the inset). In particular, in region I one finds  $T < T^{\text{ABP}}$ . For example, for  $\text{Pe}_r = 160$  the minimum at  $p = 0.4$  amounts to  $T/T^{\text{ABP}} = 0.18$ . Interestingly, this minimum occurs at a dipole strength comparable to the one estimated for *E. coli* bacteria [7].

In region II,  $T$  grows to  $10T^{\text{ABP}}$  or well beyond. The orientation of the pusher has time to equilibrate about  $\theta_s = \pi/2$  and then attempts to reach  $\theta^*$  by rotational noise. Indeed, one can rewrite the effective rotational drift in Eq. (2) by introducing an effective angular potential  $\Omega = -\partial V_{\text{eff}}/\partial\theta$  with  $V_{\text{eff}} = V + V_r = 3p \cos^2 \theta / 16 - \ln(\sin \theta) / (2\text{Pe}_r)$ , where the second term comes from the 3D rotational diffusion. However, the pusher escaping from the wall at  $\theta^*$  cannot be viewed as a typical Kramers problem [29] since the orientation vector  $\mathbf{e}$  does not pass a smooth potential barrier of height  $\Delta V_{\text{eff}}$  when reaching the escape angle  $\theta^*$ . Instead, the swimmer orientation moves up the potential  $V_{\text{eff}}$  by an amount  $\Delta V_{\text{eff}} = V_{\text{eff}}(\theta^*) - V_{\text{eff}}(\theta_s)$  and when the pusher leaves the wall at  $\theta^*$ , it also leaves the range of  $V_{\text{eff}}$  [see Fig. 3(b)]. However, we can derive an approximate formula for large  $\text{Pe}_r \Delta V_{\text{eff}}$  with the

Arrhenius factor reminiscent of Kramers' mean escape time [30,40],

$$T^{\text{pusher}} \approx \frac{\sqrt{\pi}}{|V'_{\text{eff}}(\theta^*)| \sqrt{\text{Pe}_r V''_{\text{eff}}(\theta_s)}} e^{2\text{Pe}_r \Delta V_{\text{eff}}}. \quad (6)$$

Interestingly, in case of the puller, the rotational-noise contribution  $V_r$  shifts the most stable orientation to  $\theta_s = \pi - \arcsin[2/\sqrt{-3p\text{Pe}_r}] < \pi$  [see Fig. 3(c)] [30]. Here, we can approximate  $T$  by Kramers' formula [30,41]

$$T^{\text{puller}} \approx \frac{\pi}{\sqrt{|V''_{\text{eff}}(\theta^*)| |V''_{\text{eff}}(\theta_s)}} e^{2\text{Pe}_r \Delta V_{\text{eff}}}. \quad (7)$$

The inset of Fig. 3(a) demonstrates that  $T$  calculated from Eqs. (6) and (7) at  $|p|\text{Pe}_r \gg 1$  agrees very well with the one obtained by numerically solving Eqs. (2) and (3).

While so far we considered generic microswimmer models, we now turn to the spherical *squirmers* [42], which serves as a model for ciliated microorganisms such as *Paramecium* [37,42] and *Volvox* [10] but also for active emulsion droplets [36]. The squirmer propels itself by an axisymmetric surface velocity field  $\mathbf{v}_s = \frac{3}{2}(1 + \beta \mathbf{e} \cdot \hat{\mathbf{r}}_s)[(\mathbf{e} \cdot \hat{\mathbf{r}}_s)\hat{\mathbf{r}}_s - \mathbf{e}]$ , where  $\hat{\mathbf{r}}_s$  is the unit vector pointing from the center of the squirmer to its surface. The neutral squirmer ( $\beta = 0$ ) creates the bulk flow field of a source dipole with  $q = 1/2$ , while  $\beta \neq 0$  adds an additional force-dipole field with  $p = -3\beta/4$  [43]. Recent studies with squirmer-wall interactions already exist but without any noise [15,22,23,44]. Using lubrication theory, the authors of Ref. [43] have calculated the dimensionless friction torque acting on the squirmer in front of a wall due to hydrodynamic interactions [43],

$$M = (6\pi/5)(1 - \beta \cos \theta) \sin \theta (\ln \epsilon^{-1} - c), \quad (8)$$

where  $\epsilon = h - 1 \ll 1$  is a small distance and  $c = \text{const}$ . This gives the wall-induced angular velocity  $\Omega_{\text{HI}} = -M/\gamma_r$ , where  $\gamma_r$  is the rotational friction coefficient near the surface [45,46]. Note that the neutral squirmer ( $\beta = 0$ ) behaves like the generic source dipole even close to the wall since  $\Omega_{\text{HI}} \sim -\sin \theta$ . This might explain why far-field hydrodynamic interactions describe the near-wall swimming of neutral squirmers as shown in Ref. [15]. The  $\beta$ -dependent part in Eq. (8) adds to  $\Omega_{\text{HI}}$  the force-dipole term  $\sim -p \sin \theta \cos \theta$ . Acting alone, it rotates the squirmer pusher ( $\beta < 0$ ) towards the wall and therefore it behaves like the generic puller with increased detention time and vice versa. These results are in accordance with recent simulations at finite Reynolds numbers [23].

To demonstrate that our 1D model is applicable, we perform full 3D mesoscale hydrodynamic simulations using multiparticle collision dynamics (MPCD) [47–49]. It solves the Navier-Stokes equations for the fluid around the squirmer and the wall and naturally includes thermal

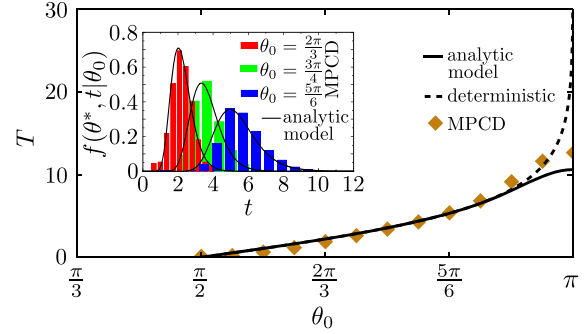


FIG. 4 (color online). Mean detention time  $T$  of a neutral squirmer plotted versus the initial angle  $\theta_0$  for  $\text{Pe}_r = 110$  and  $\epsilon = 0.01$  (approximate mean distance from the wall measured from MPCD simulations) and compared to the analytic 1D model [Eqs. (2) and (3)], and the deterministic model ( $\text{Pe}_r \rightarrow \infty$ ). Inset: Distribution of detention times from MPCD simulations and compared to the analytic model.

fluctuations [50–53]. First, we numerically determine  $c \approx 0.9$  [30] and then explicitly simulate many swimming trajectories of swimmer-wall collision events for a neutral squirmer at different incoming angles. Figure 4 shows results for the mean detention time  $T$  plotted versus the initial angle  $\theta_0$ , which agree well with our analytic model. The mean detention time of the deterministic swimmer,  $T^{\text{det}} \propto \ln \tan(\theta_0/2)$  [30], deviates from the full model only close to the unstable equilibrium orientation at  $\theta = \pi$ . Here  $T^{\text{det}} \rightarrow \infty$ , whereas noise renders  $T$  finite and helps the swimmer to escape. The inset of Fig. 4 shows a convincing agreement of the DTDs determined from the analytic model and MPCD simulations.

To assess fluctuations of the position  $h(t)$  above the surface, which influence  $\Omega_{\text{HI}}$  [8,54], we may define an escape event by reaching a certain escape height  $h^* > 1$ . For the state variable  $\mathbf{y}(t) = (h, \theta)$  one defines the probability  $g(\mathbf{y}^*, t|\mathbf{y}_0)$ , for finding the swimmer below  $h^*$  at time  $t = t^* - t_0$  while the initial state  $\mathbf{y}_0$  at  $t_0$  starts at  $h_0 \in [1, h^*)$  and  $\theta_0 \in [0, \pi]$  [55]. The probability obeys the adjoint Fokker-Planck equation

$$\begin{aligned} \partial_t g(\mathbf{y}^*, t|\mathbf{y}_0) = & [(\mathbf{v}_A + \mathbf{v}_{\text{HI}}) \cdot \mathbf{e}_z \partial_{h_0} + D_t \partial_{h_0}^2 \\ & - (\Omega_{\text{HI}} + D_r \cot \theta_0) \partial_{\theta_0} + D_r \partial_{\theta_0}^2] g(\mathbf{y}^*, t|\mathbf{y}_0), \end{aligned} \quad (9)$$

with the initial condition  $g(\mathbf{y}^*, t_0|\mathbf{y}_0) = \delta(\mathbf{y}^* - \mathbf{y}_0)$ , and reflecting [at  $\mathbf{y}_0 = (1, \pi)$ ] and absorbing [at  $\mathbf{y}_0 = (h^*, \theta^*)$ ] boundary conditions for  $g(\mathbf{y}^*, t|\mathbf{y}_0)$ . Then,  $f(\mathbf{y}^*, t|\mathbf{y}_0) = -\partial_t g(\mathbf{y}^*, t|\mathbf{y}_0)$  is the DTD for detention time  $t$ . In Ref. [30] we show that for sufficiently large  $\text{Pe}$  and  $h^*$  the detention times in the 2D model are larger compared to the 1D model. Small  $h^*$  can also be reached by translational Brownian motion, which reduces the detention times.

To conclude, based on the method of first-passage times, we developed a formalism to determine the distribution of detention times for microswimmers near a plane no-slip surface taking into account hydrodynamic interactions and rotational noise. For generic microswimmers such as source dipoles, pushers, and pullers we demonstrated that the mean detention time can vary over several orders of magnitude relative to the ABP depending on persistence number  $Pe_r$  and swimmer strengths  $q$ ,  $p$ . This allows us to quantify the relative importance of hydrodynamic interactions and rotational noise. Our model also provides a route to quantify wall accumulation of microswimmer suspensions confined between two plates, as determined experimentally for different microorganisms [8,11,13,56]. Our method can be extended to include further drift terms, for example, due to nonspherical swimmer shape, which further modifies the reorientation dynamics at the wall [11,15]. Therefore, it offers a systematic approach for studying how artificial as well as biological microswimmers behave at surfaces.

We thank Giovanni Volpe and Katrin Wolff for helpful discussions and the Deutsche Forschungsgemeinschaft for financial support within the research training group GRK 1558, within the priority program SPP 1726 “Microswimmers” (STA 352/11), and by Grant STA 352/10-1.

- 
- [1] H. C. Berg, *Random Walks in Biology* (Princeton University Press, Princeton, NJ, 1993).
- [2] E. Lauga and T. R. Powers, The hydrodynamics of swimming microorganisms, *Rep. Prog. Phys.* **72**, 096601 (2009).
- [3] D. Bray, *Cell Movements* (Garland, New York, 2000).
- [4] M. E. Callow and J. A. Callow, Marine biofouling: A sticky problem, *Biologist* **49**, 1 (2002).
- [5] E. Rosenberg, O. Koren, L. Reshef, R. Efrony, and I. Zilber-Rosenberg, The role of microorganisms in coral health, disease and evolution, *Nat. Rev. Microbiol.* **5**, 355 (2007).
- [6] P. Watnick and R. Kolter, Biofilm, city of microbes, *J. Bacteriol.* **182**, 2675 (2000).
- [7] K. Drescher, J. Dunkel, L. H. Cisneros, S. Ganguly, and R. E. Goldstein, Fluid dynamics and noise in bacterial cell-cell and cell-surface scattering, *Proc. Natl. Acad. Sci. U.S.A.* **108**, 10940 (2011).
- [8] A. P. Berke, L. Turner, H. C. Berg, and E. Lauga, Hydrodynamic Attraction of Swimming Microorganisms by Surfaces, *Phys. Rev. Lett.* **101**, 038102 (2008).
- [9] E. Lauga, W. R. DiLuzio, G. M. Whitesides, and H. Stone, Swimming in circles: Motion of bacteria near solid boundaries, *Biophys. J.* **90**, 400 (2006).
- [10] K. Drescher, K. C. Leptos, I. Tual, T. Ishikawa, T. J. Pedley, and R. E. Goldstein, Dancing Volvox: Hydrodynamic Bound States of Swimming Algae, *Phys. Rev. Lett.* **102**, 168101 (2009).
- [11] G. Li and J. X. Tang, Accumulation of Microswimmers near a Surface Mediated by Collision and Rotational Brownian Motion, *Phys. Rev. Lett.* **103**, 078101 (2009).
- [12] V. Kantsler, J. Dunkel, M. Polin, and R. E. Goldstein, Ciliary contact interactions dominate surface scattering of swimming eukaryotes, *Proc. Natl. Acad. Sci. U.S.A.* **110**, 1187 (2013).
- [13] M. M. Molaei, M. Barry, R. Stocker, and J. Sheng, Failed Escape: Solid Surfaces Prevent Tumbling of *Escherichia coli*, *Phys. Rev. Lett.* **113**, 068103 (2014).
- [14] I. Jung, K. Guevorkian, and J. M. Valles, Trapping of Swimming Microorganisms at Lower Surfaces by Increasing Buoyancy, *Phys. Rev. Lett.* **113**, 218101 (2014).
- [15] S. E. Spagnolie and E. Lauga, Hydrodynamics of self-propulsion near a boundary: Predictions and accuracy of far-field approximations, *J. Fluid Mech.* **700**, 105 (2012).
- [16] W. R. DiLuzio, L. Turner, M. Mayer, P. Garstecki, D. W. Weibel, H. C. Berg, and G. M. Whitesides, *Escherichia coli* swim on the right-hand side, *Nature (London)* **435**, 1271 (2005).
- [17] D. Takagi, J. Palacci, A. B. Braunschweig, M. Shelley, and J. Zhang, Hydrodynamic capture of microswimmers into sphere-bound orbits, *Soft Matter* **10**, 1784 (2014); S. E. Spagnolie, G. R. Moreno-Flores, D. Bartolo, and E. Lauga, Geometric capture and escape of a microswimmer colliding with an obstacle, *Soft Matter* **11**, 3396 (2015).
- [18] G. Volpe, I. Buttinoni, D. Vogt, H.-J. Kümmerer, and C. Bechinger, Microswimmers in patterned environments, *Soft Matter* **7**, 8810 (2011).
- [19] C. Kreuter, U. Siems, P. Nielaba, P. Leiderer, and A. Erbe, Transport phenomena and dynamics of externally and self-propelled colloids in confined geometry, *Eur. Phys. J. Spec. Top.* **222**, 2923 (2013).
- [20] D. G. Crowdy and Y. Or, Two-dimensional point singularity model of a low-Reynolds-number swimmer near a wall, *Phys. Rev. E* **81**, 036313 (2010).
- [21] D. G. Crowdy, Wall effects on self-diffusiophoretic Janus particles: A theoretical study, *J. Fluid Mech.* **735**, 473 (2013).
- [22] K. Ishimoto and E. A. Gaffney, Squirmer dynamics near a boundary, *Phys. Rev. E* **88**, 062702 (2013).
- [23] G.-J. Li and A. M. Ardekani, Hydrodynamic interaction of microswimmers near a wall, *Phys. Rev. E* **90**, 013010 (2014).
- [24] W. E. Uspal, M. N. Popescu, S. Dietrich, and M. Tasinkevych, Self-propulsion of a catalytically active particle near a planar wall: from reflection to sliding and hovering, *Soft Matter* **11**, 434 (2015).
- [25] S. van Teeffelen and H. Löwen, Dynamics of a Brownian circle swimmer, *Phys. Rev. E* **78**, 020101(R) (2008).
- [26] M. Enculescu and H. Stark, Active Colloidal Suspensions Exhibit Polar Order under Gravity, *Phys. Rev. Lett.* **107**, 058301 (2011).
- [27] C. F. Lee, Active particles under confinement: aggregation at the wall and gradient formation inside a channel, *New J. Phys.* **15**, 055007 (2013).
- [28] J. Elgeti and G. Gompper, Wall accumulation of self-propelled spheres, *Europhys. Lett.* **101**, 48003 (2013).
- [29] J. Honerkamp, *Stochastic Dynamical Systems* (VCH, New York, 1994), Chaps. 6 and 9.
- [30] See Supplemental Material at <http://link.aps.org/supplemental/10.1103/PhysRevLett.115.038101> for additional information on the adjoint Smoluchowski equation, the calculation of mean detention times, swimming near a

- wall, an estimation of translational escape times, a comparison of our 1D with our 2D model, DTDs for a simple *Chlamydomonas* model, and the angular velocity  $\Omega(\theta, \epsilon)$  for a neutral squirmer near a wall determined from MPCD simulations.
- [31] The escape from a surface is indeed mainly determined by rotational motion; see Ref. [30].
- [32] K. Wolff, A. M. Hahn, and H. Stark, Sedimentation and polar order of active bottom-heavy particles, *Eur. Phys. J. E* **36**, 43 (2013).
- [33] J. Taktikos, V. Zaburdaev, and H. Stark, Collective dynamics of model microorganisms with chemotactic signaling, *Phys. Rev. E* **85**, 051901 (2012).
- [34] B. M. Friedrich and F. Jülicher, Steering Chiral Swimmers along Noisy Helical Paths, *Phys. Rev. Lett.* **103**, 068102 (2009).
- [35] B. J. Berne and R. Pecora, *Dynamic Light Scattering* (Dover, New York, 2000), Chap. 7.
- [36] S. Thutupalli, R. Seemann, and S. Herminghaus, Swarming behavior of simple model squirmers, *New J. Phys.* **13**, 073021 (2011).
- [37] T. Ishikawa and M. Hota, Interaction of two swimming Paramecia, *J. Exp. Biol.* **209**, 4452 (2006).
- [38] We note that swimmer flow fields and, hence,  $\Omega_{HI}$  can be time dependent [39] and may influence the DTDs, which we neglect in the following.
- [39] K. Drescher, R. E. Goldstein, N. Michel, M. Polin, and I. Tuval, Direct Measurement of the Flow Field around Swimming Microorganisms, *Phys. Rev. Lett.* **105**, 168101 (2010); J. S. Guasto, K. A. Johnson, and J. P. Gollub, Oscillatory Flows Induced by Microorganisms Swimming in Two Dimensions, *ibid.* **105**, 168102 (2010).
- [40] For an alternative, heuristic expression based on Kramers theory see Ref. [7].
- [41] See Ref. [30] for the limit  $|p|Pe_r \rightarrow \infty$ .
- [42] J. Lighthill, On the squirming motion of nearly spherical deformable bodies through liquids at very small Reynolds numbers, *Commun. Pure Appl. Math.* **5**, 109 (1952); J. R. Blake, A spherical envelope approach to ciliary propulsion, *J. Fluid Mech.* **46**, 199 (1971).
- [43] T. Ishikawa, M. P. Simmonds, and T. J. Pedley, Hydrodynamic interaction of two swimming model micro-organisms, *J. Fluid Mech.* **568**, 119 (2006).
- [44] I. Llopis and I. Pagonabarraga, Hydrodynamic interactions in squirmer motion: Swimming with a neighbour and close to a wall, *J. Non-Newtonian Fluid Mech.* **165**, 946 (2010).
- [45] B. Cichocki and R. B. Jones, Image representation of a spherical particle near a hard wall, *Physica (Amsterdam)* **258A**, 273 (1998).
- [46] We neglect here the small translational-rotational coupling.
- [47] A. Malevanets and R. Kapral, Mesoscopic model for solvent dynamics, *J. Chem. Phys.* **110**, 8605 (1999).
- [48] R. Kapral, Multiparticle collision dynamics: simulation of complex systems on mesoscales, *Adv. Chem. Phys.* **140**, 89 (2008).
- [49] G. Gompper, T. Ihle, D. M. Kroll, and R. G. Winkler, Multiparticle collision dynamics: A particle-based Mesoscale simulation approach to the hydrodynamics of complex fluids, *Adv. Polym. Sci.* **221**, 1 (2009).
- [50] M. T. Downton and H. Stark, Simulation of a model microswimmer, *J. Phys. Condens. Matter* **21**, 204101 (2009).
- [51] I. O. Götze and G. Gompper, Mesoscale simulations of hydrodynamic squirmer interactions, *Phys. Rev. E* **82**, 041921 (2010).
- [52] A. Zöttl and H. Stark, Nonlinear Dynamics of a Microswimmer in Poiseuille Flow, *Phys. Rev. Lett.* **108**, 218104 (2012).
- [53] A. Zöttl and H. Stark, Hydrodynamics Determines Collective Motion and Phase Behavior of Active Colloids in Quasi-Two-Dimensional Confinement, *Phys. Rev. Lett.* **112**, 118101 (2014).
- [54] G. Li, L.-K. Tam, and J. X. Tang, Amplified effect of Brownian motion in bacterial near-surface swimming, *Proc. Natl. Acad. Sci. U.S.A.* **105**, 18355 (2008).
- [55] K. Schaar, Master's thesis, Technische Universität Berlin, 2013.
- [56] L. Rothschild, Non-random distribution of bull spermatozoa in a drop of sperm suspension, *Nature (London)* **198**, 1221 (1963).